

## STABILITY OF VISCOELASTIC LIQUID CURTAIN

Melisa Z. Becnerra, melisa@aluno.puc-rio.br

Marcio S. Carvalho, msc@puc-rio.br

Department of Mechanical Engineering - Pontificia Universidade Catolica de Rio de Janeiro  
R. Marques de São Vicente 225- Gávea, Rio de Janeiro, RJ, Brasil

**Abstract.** *Thin liquid sheets occur in numeral practical applications, such as curtain coating and atomization processes. In the particular case of curtain coating, a thin liquid sheet is formed and falls freely over a considerable height before it impinges onto the substrate to be coated. One of the important limitations of this process is the stability of the liquid curtain, which may define the minimal thickness that can be coated at a given web speed. The conditions at which a low viscosity Newtonian liquid curtain breaks was derived based on simple balance between inertial and capillary forces by Brown (1961). For viscoelastic liquids, the normal tensile stress related to stretching of the polymer molecules as the liquid accelerates down the curtain changes the force balance. In this research, the critical condition at which a viscoelastic liquid curtain breaks was determined as a function of the rheological properties of the coating liquid. The results show that high extensional viscosity liquids creates more stable curtains. Liquid additives could be used in order to push limits of curtain flow rate to smaller values and consequently to widen the operability window of the process.*

**Keywords:** *curtain coating, curtain break up, viscoelastic liquids*

### 1. INTRODUCTION

Curtain coating is one the preferred methods for precision coating and has been used to manufacture single and, most notably, multilayer coatings and patch coatings on substrates or webs moving at relatively high speeds. Liquid falls as a sheet, or curtain, freely over a considerable height and under the action of gravity before it impinges onto the substrate being coated (Kistler and Schweizer, 1997). Precision curtain coating was originally developed for multilayer photographic film but its use has expanded to many different applications such as optical films and specialty papers. Some advantages of this process include very high coating speeds, adaptability to a wide range of liquids and flexibility to apply thin liquid layer to irregular surfaces. In this process, the flow can be divided into several subregions to systematically analyze the flow dynamics of this process; one of these subregions is the curtain flow region beyond the lip where the falling liquid experiences uniaxial extensional deformation by gravity force. One of the operability limits of the process is set by curtain break up for the curtain flow region.

In this work, we focus in the curtain flow region. Both the interfacial shape and the stability of liquid sheets have been investigated before. As first pointed out by Squire (1953), the sheet break-up results from the growth of transverse waves. Two kinds of waves are possible at any given frequency: either the two free surfaces of the sheet are both displaced in the same direction to form sinuous waves, or they moves in opposite directions, as in varicose waves. Experimentally, one of the first noticeable contributions was brought on by Brown (1961), who studied the shape and stability of a curtain falling over a moving surface (which mimics a coating processes). He suggested that a simple stability criterion could be built by comparing the momentum flux  $\rho h U^2$  pushing downstream possible transient holes ( $\rho$  is liquid density,  $h$  is local curtain thickness, and  $U$  is local fluid velocity) with twice the surface tension  $\gamma$ , that tends to pull the hole upstream. This balance naturally introduces the Weber number  $We = \rho h U^2 / \gamma$  or  $We = \rho q U / \gamma$  as a key parameter for curtain stability. Brown's (1961) conclusions were that the Weber number had to be larger than 2 to prevent any curtain break-up, in other words if the flow rate is decreased below a certain value, the curtain tends to break up, and individual fluid columns appears as shown in Fig.1. His pioneering physical interpretation remains a milestone for modern theoretical and numerical investigations. Critical flow rates for the transitions between different flow regimes were determined experimentally, for instance, by Limat *et al.* (1992) and Hu and Jacobi (1996).

The rupture of a falling curtain may be initiated near the edge guides, or inside the curtain, away from the edges, through the generation of holes by impurities (aerosol droplets or dust particles). While the mechanism of rupture near the edge guides is certainly important, it is more difficult to analyze, compared to that originating in local sheet defects, for which an infinitely extended sheet (in transverse direction) could provide an adequate model. But even the sheet rupture through the local generation and growth of a hole is not satisfactorily clarified at present, despite experimental analysis as Finnium *et al.* (1993) and Luca (1999), and theoretical studies as Lin (1990), Luca (1997) and Teng (1997) studies, mainly due to the strong nonlinearity involved in this process.

If the viscosity of the liquid is large enough, viscous tensile stresses in the curtain cannot be neglected, as done in the simple model of Brown (1961). Sünderhauf (2002) shows that the viscous forces decelerate the growth of a hole in the curtain, leading to smaller minimum flow rate. If the liquid presents viscoelastic stress, the force balance becomes even more complex.

The goal of this work is to study experimentally the effect of a high molecular weight polymer in dilute regime in the critical flow rate curtain break up.

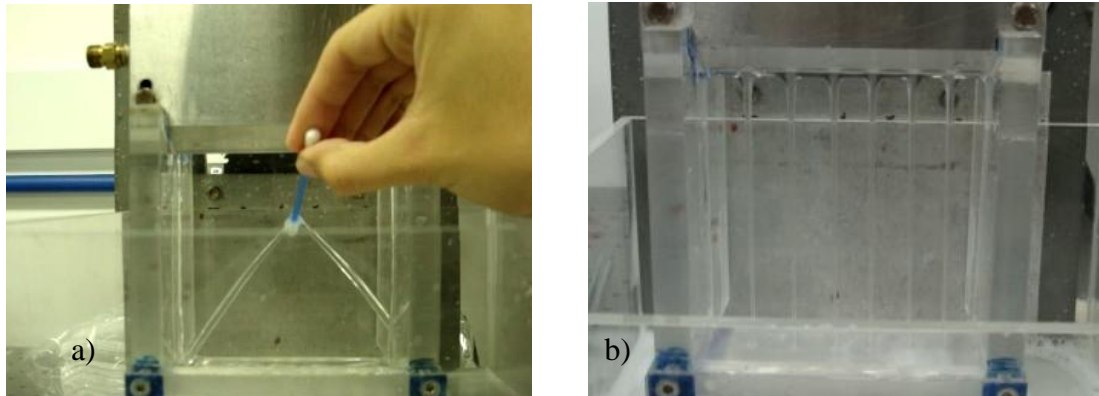


Figure 1. a) Perturbed curtain, b) Completely disintegrated curtain.

## 2. EXPERIMENTAL ANALYSIS

### 2.1. Experimental set up and procedure

The experiments were conducted in the test section shown schematically in Fig. 2. The liquid flows from a reservoir (a), through a gear pump (COLE-PALMER 75211-60) (b), which imposes a constant flow rate  $Q$ . A half-filled chamber (c) damps residual pulsation caused by the pump. The flow rate is controlled by the pump speed and measured by a Coriolis meter (MICRO MOTION model CMF025) (d). The liquid is then supplied to a plastic tube ( $d = 0,25$  inch) to feed to coating die from which the liquid flows. The coating die, width equal to 100mm, was assembled with shims such that the gap of the slot was  $100 \mu\text{m}$ . If the flow rate is sufficiently high, a liquid curtain is formed and it is kept from contracting towards the center by two slightly convergent acrylic plates (e). The height of the curtain was constant and equal to 100 mm. The liquids remain at room temperature during the experiments, about  $23^\circ\text{C}$  and is necessary to prevent air motions around the experiment to avoid perturbations in the curtain liquid.

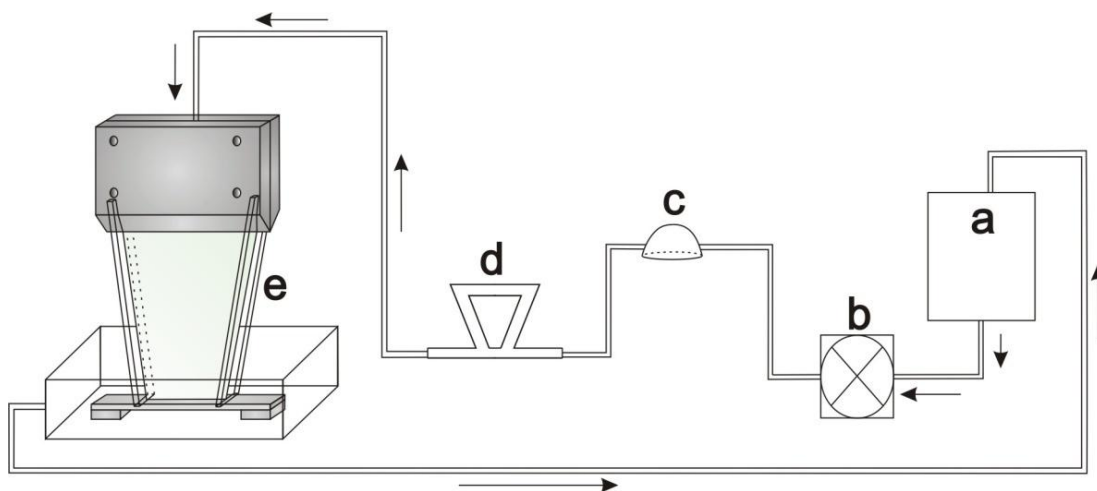


Figure 2. Sketch of the experiment

The minimum flow rate that could be used to get a stable curtain was found by the following procedure:

- (1) The pump speed was set to deliver high enough flow rate to obtain a very stable curtain, we waited a few minutes to stabilize the flow.
- (2) The pump speed was lowered in small steps. After less than 60 seconds, steady state was reached for each step. The flow rate was lowered until the curtain breaks. Detail of how curtain break-up are described in the subsequent section.

### 2.2 Solutions and rheological characterization

The coating liquids used in the experiments were solutions of polyethylene glycol (molecular weight  $6 \times 10^3$  g/mol) and polyethylene oxide (molecular weight  $8 \times 10^6$  g/mol). These aqueous polymer solutions were proposed by Dontula *et al.* (1998) as model liquids to study the role of elasticity in coating and other free surface flows. These solutions are transparent and behave as Boger liquids. The solution of low molecular weight PEG in water was used as the "solvent"

to all liquids tested. Because of the low molecular weight, the solution of PEG in water is Newtonian. Their rheological properties depended on concentration. The concentration of the PEG was fixed at 20 wt%, which yielded a viscosity of approximately 10 cP. To reduce the surface tension surfactant; sodium dodecyl sulfate (SDS), was added in the solutions. The concentration used was 2.77 mM, less than the critical aggregation concentration (CAC) at which surfactant first begins to aggregate with the polymer (PEO) as explained by Ergungor *et al.* (2006). The addition of small quantities of the high molecular weight PEO made the solutions elastic. The concentration of PEO varied from 0 to 0.3 wt%.

The rheological characterization of the solutions was made in shear and extension-dominated flows. The rheological properties in shear were obtained using a rotational rheometer (Physica MCR Rheometer, Anton-Paar) with a Couette fixture (1), and a Cannon-Fenske glass capillary rheometer (2) in order to determine the inherent viscosity of the solutions tested as a function of the PEO concentration with higher accuracy at low shear rate. The shear viscosity of all solutions tested is independent of the shear rate, as shown in Fig. 3, indicating that at this level of concentration of PEO, the solutions were in the dilute regime, with the exception of the last one that had a slight shear thinning behavior.

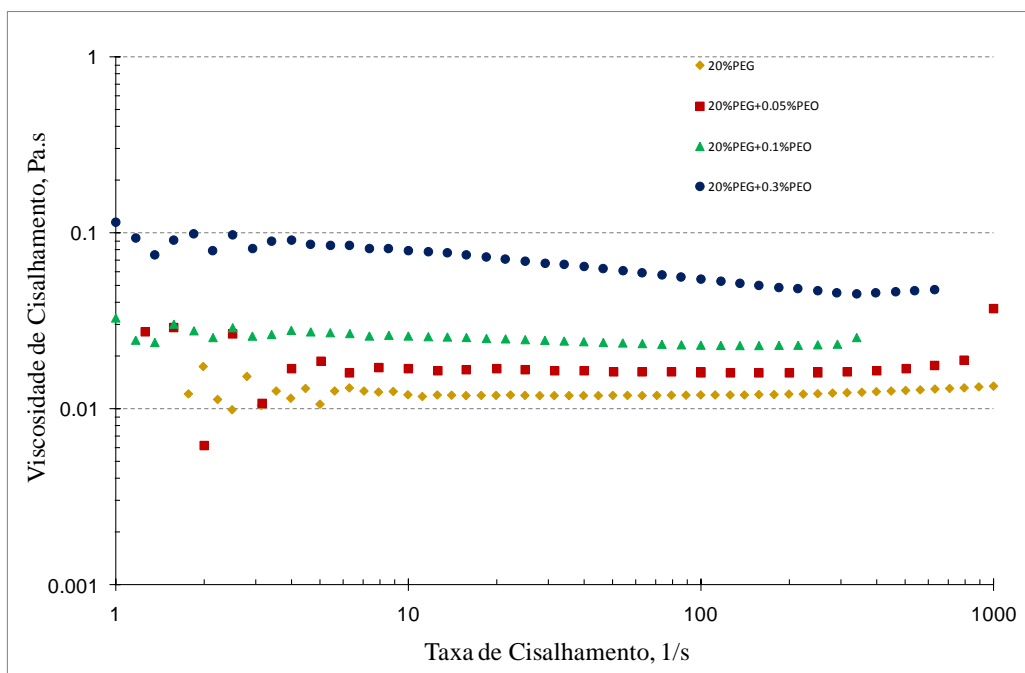


Figure 3. Shear viscosity dependence on shear rate

Table 1 presents the viscosity of the solutions at different PEO concentration (from 0 to 0.3 wt.%) in 20 wt.% PEG solutions. The variation of the inherent viscosity, defined as  $(\eta_0 - \eta_s)/\eta_s$  with PEO concentration is presented in Fig. 4. It is independent of the PEG concentration and varies linearly with the high molecular weight polymer (PEO) concentration. The last solution is out of this linear behavior. The intrinsic viscosity, i.e. the slope of the line, is approximately  $[\eta] \approx 0.7 \text{ m}^3/\text{kg}$ . At equilibrium, the polymer coils start to overlap when the reduced concentration, defined as  $c^* = c/[\eta]$ , is approximately  $c^* = 1$ , as discussed by Macosko (1994). The maximum reduced concentration of the solutions tested here was below this limit and consequently all the test liquids were in the dilute regime, except the last solution. The relaxation time of the solutions were estimated by taking  $\lambda \equiv \eta_p/G$ , where  $\eta_p$  is the polymer contribution for the viscosity ( $\eta_p = \eta_0 - \eta_s$ ) and  $G$  is the elastic modulus of the liquid. It is a function of the polymer concentration  $c$  and its molecular weight  $M_w$  ( $G \equiv (c/M_w)RT$ ). The estimated relaxation time of each solution is also presented in Tab. 1. As expected in the dilute regime, the relaxation time is independent of the PEO concentration. The estimated relaxation time was  $\lambda \approx 0.02 \text{ s}$  for the 20 wt.% PEG solution.

Table1. Estimated relaxation time of solution, different PEO concentration

PEG (% wt)	PEO (% wt)	$\rho$ (kg/m <sup>3</sup> )	$c$ (kg/m <sup>3</sup> )	$\eta_0$ (1) (Pa.s)	$\eta_0$ (2) (Pa.s)	$\eta_s$ (Pa.s)	$\eta_p$ (Pa.s)	$(\eta_0 - \eta_s)/\eta_s$	$G$ (Pa)	$\lambda$ (s)
20	0	1031.8	0	0.0122	0.0125	0.0125	0.0000	0.0004	0.000	0.0000
	0.05	1032.2	0.5161	0.0177	0.0165	0.0125	0.0039	0.3118	0.213	0.0183
	0.1	1032.7	1.0327	0.0255	0.0217	0.0125	0.0092	0.7315	0.426	0.0215
	0.3	1033.5	3.1005	0.0684	0.0572	0.0125	0.0446	3.5572	1.280	0.0348

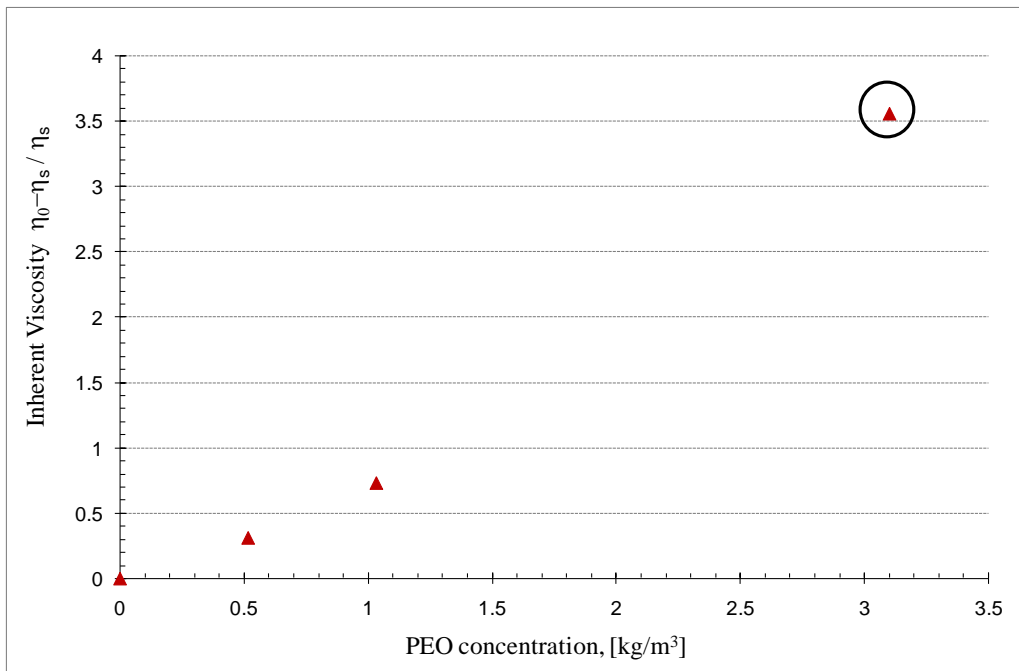


Figure 4. Inherent viscosity  $(\eta_0 - \eta_s)/\eta_s$  as a function of PEO concentration

The apparent extensional viscosity was measured using a capillary thinning extensional rheometer (CABER, Thermo Fisher Scientific). In this technique, a liquid bridge of the test fluid is formed between two cylindrical test fixtures as indicated schematically in Fig. 5a. An axial step-strain is then applied, which results in the formation of elongated liquid thread. The instrument uses a laser micrometer to monitor the diameter of a thinning filament. The evolution in the mid-point diameter, for the three non-Newtonian solutions, is plotted versus time in Fig. 5b. As expected, the solution with high concentration of PEO, more elastic, has a late filament break up. The Newtonian solution takes a very short time to break up so it is hard for the instrument to get enough data from this case.

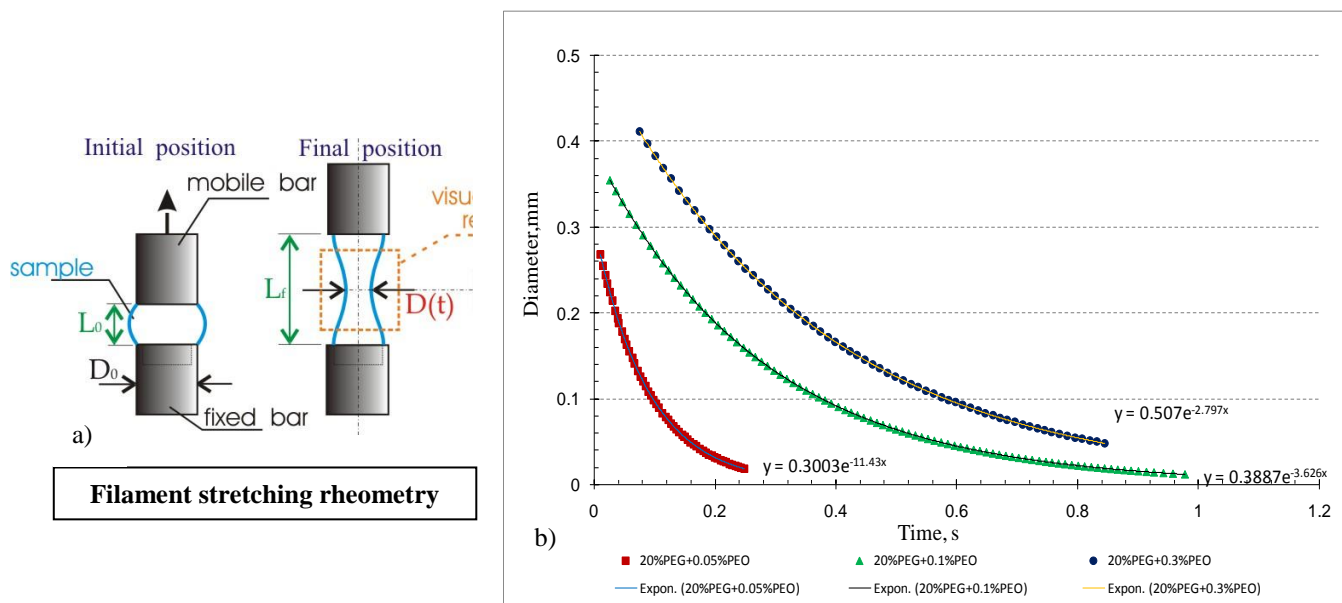


Figure 5. a) Esqueme of filament stretching, b) Diameter of filament as function of time

Figure 5 shows that following a rapid initial viscous-dominated phase, there is an intermediated time in which the dynamics of filament drainage are governed by balance between surface tension and elasticity, rather than the fluid viscosity. In this regime, the filament radius decrease exponentially as Eq. (1), where  $\lambda$  is the relaxation time governing the capillary break up and  $G$  is the elastic modulus of the filament.

$$D_{mid}(t) = D_0 \left[ \frac{GD_0}{\sigma} \right]^{1/3} e^{-t/3\lambda} \quad (1)$$

This evolution is driven by the capillary pressure and resisted by the extensional stress in the fluid. The measurements can thus also be represented in terms of an apparent extensional viscosity, which is defined by Eq.(2):

$$\eta_{app}(\varepsilon) = \frac{2\sigma/D_{mid}(t)}{\left\{ -\frac{2}{D_{mid}} \frac{dD_{mid}}{dt} \right\}} = \frac{\sigma}{\frac{dD_{mid}}{dt}}, \quad (2)$$

and the Hencky strain is defined as Eq.(3):

$$\varepsilon = \ln(D_{mid}(t)/D_0) = -\frac{2}{D_{mid}} \frac{dD_{mid}}{dt} \quad (3)$$

Then the data can be replotted in the form of an extensional viscosity as shown in Fig.6.

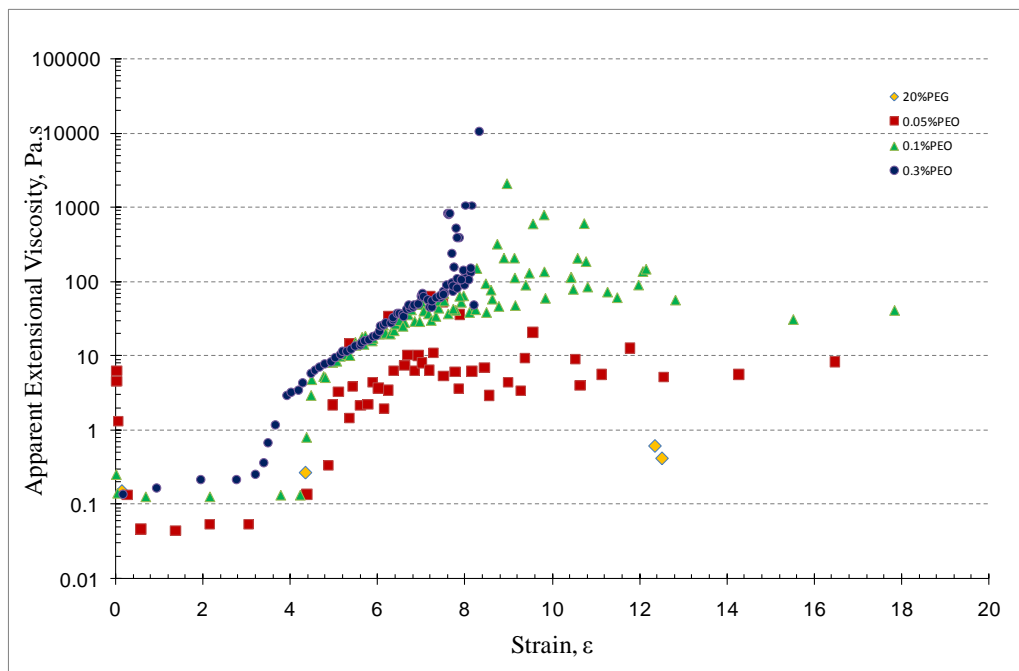


Figure 6. Apparent extensional viscosity versus strain

In the solution lacking PEO, a Newtonian solution, the apparent extensional viscosity is virtually independent of the extensional rate. The measured *Trouton* ratio is approximately  $\eta_e/\eta_s \approx 8$ . It is important to notice that the number of data points obtained for the Newtonian liquid is very small because the filament breaks in an extremely short time, as mentioned

For the viscoelastic solutions, the apparent extensional viscosity varies with the extensional strain, as expected. At low strain, it is approximately equal to the Newtonian solution. It rises sharply at  $3 < \varepsilon < 5$  to the value at high strain. At a concentration of 0.05% PEO, the measured *Trouton* ratio at high strains is approximately  $\eta_e/\eta_s \approx 500$ . The apparent extensional viscosity at high strains rises with the high molecular weight polymer concentration.

### 3. Results

The experiments offered an overview of the curtain responses to the rheological properties of the solutions. Figure 7 shows that the curtain destruction results from amplification of a local and transient hole on the curtain. A free edge (hole) appears at the bottom, climbs up and finally invades the entire curtain, that is disintegrated in small liquid columns, like was reported by Roche *et al.* (2006). This is independent of the rheological properties of the solutions. The critical Weber number,  $We = qV/2\sigma$ , was calculated from this minimal flow rate and plotted versus the PEO concentration in the solutions, as is shown in Fig.8.

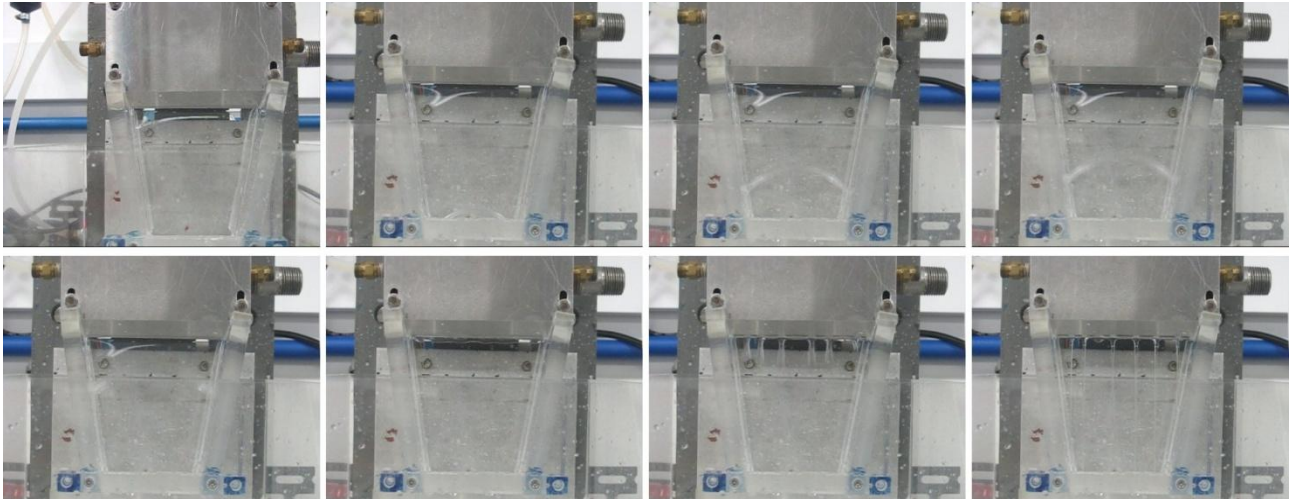


Figure 7. Sequence of evolution the curtain break up

The critical Weber number for the Newtonian liquid was approximately  $We \approx 1.2$ , which is smaller than the critical value of  $We=2$  proposed by Brown (1961). The reason is that the liquid viscosity  $\eta \approx 0.0122$  Pa.s is such that the viscous normal stress resists the retraction of the hole up the curtain leading to smaller values of the minimum flow rate.

The critical Weber numbers falls as the PEO concentration rises, i.e., the elasticity of the solution stabilizes the curtain. This result clearly shows that the elastic properties of the coating liquid can reduce the minimal flow rate to break the curtain by more than 50%.

Sünderhauf (2002) made the first study of the role played by the viscosity in the stability of a liquid curtain. His conclusion was that the critical Weber number is inversely proportional to the viscosity of the solution, so the higher viscosity the smaller is the critical Weber number. With this background we can presume that in our case when, we are increasing the PEO concentration, we actually stabilize the liquid curtain by increasing the “extensional viscosity” of the solution, as shown the Fig. 9

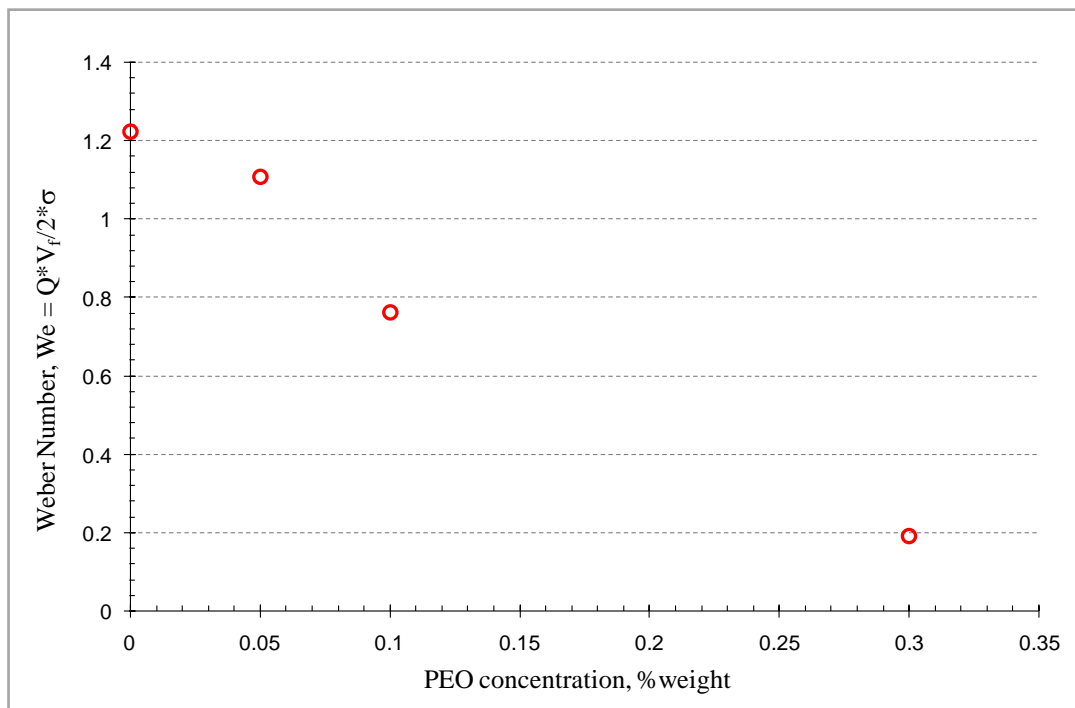


Figure 8. Critical Weber Number versus PEO concentration

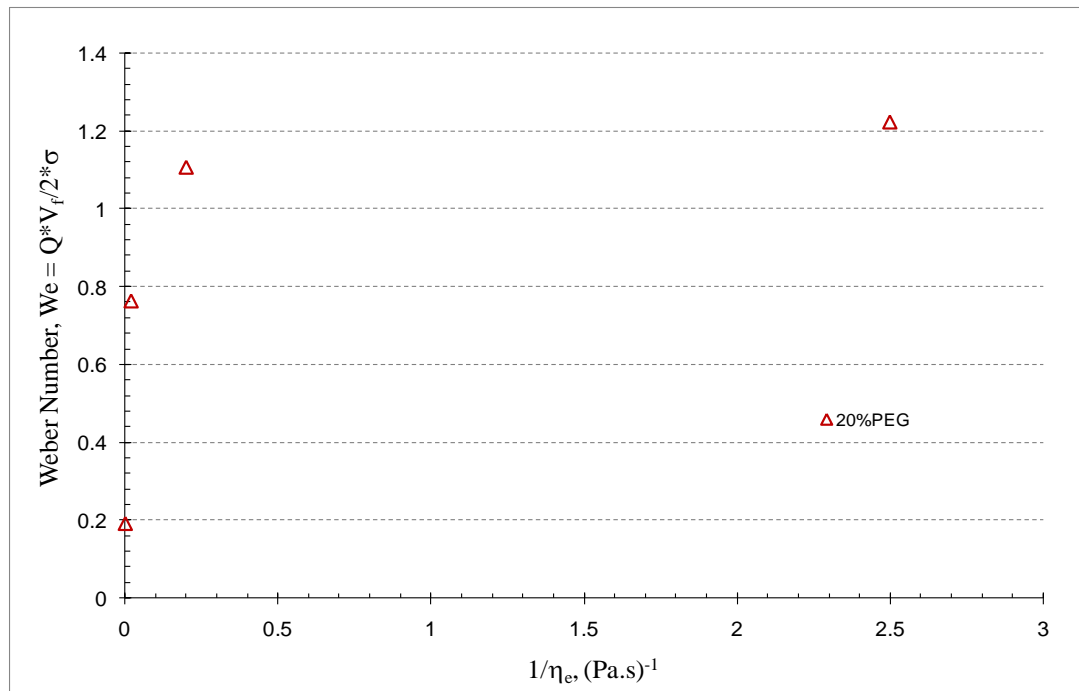


Figure 9. Critical Weber number versus inverse of the extensional viscosity

#### 4. FINAL REMARKS

The results show that the minimum flow rate necessary to keep a liquid curtain stable, which limits the applicability of the curtain coating, can be drastically reduced by changing the rheological response of the coating liquid. One possibility is to raise the extensional viscosity of the liquid by adding small amounts of a high molecular weight polymer. By doing so, the shear viscosity of the liquid does not change much, keeping the pressure drop in the feeding system, pressure inside the die and leveling characteristics almost the same. The effect is restricted to the flow region dominated by extensional deformation, i.e., the falling curtain.

#### 5. ACKNOWLEDGEMENTS

M. Z. B. was supported with a scholarship from the “*Fundação Carlos Chagas Filho de Amparo à Pesquisa do Estado do Rio de Janeiro*” (Faperj). This work was partially funded by HP (USA).

#### 6. REFERENCES

- Brown D. R., 1961 “A study of the behavior of a thin sheet of a moving liquid”, *Journal Fluid Mechanics*, Vol. 10, 297-305 p.
- De Luca L., 1999, “Experimental investigation of the global instability of plane sheet flows”, *Journal Fluid Mechanics*, Vol. 399, 355-376 p.
- De Luca L. and Costa M., 1997, “Instability of spatially developing liquid sheet”, *Journal Fluid Mechanics*, Vol. 331, 127-144 p.
- Dontula P., Macosko C.W., Scriven L.E., 1998, “Model Elastic Liquids with Water Soluble Polymer”, *AIChE J.*, Vol. 44, 1247–1255 p.
- Ergungor Z., Smolinski J. M., Manke C. W. and Gulari E., 2006, “Effect of polymer-surfactant interactions on elongational viscosity and atomization of peo solutions”, *Journal of Non-Newtonian Fluid Mechanics*, Vol. 138, 1-6p.
- Hu X. and Jacobi A.M., 1996, “The intertube falling film: Part 1-flow characteristics, mode transitions, and hysteresis”, *Trans. ASME, Ser. C: J. Heat Transfer*, Vol. 118, 616-625 p.
- Klister F. and Schweizer P. M., 1997, “Curtain coating,” in *Liquid Film coating*, edited by Chapman & Hall, London, 463-494 p.
- Finnicum D. S., Weinstein S. J., and Ruschak K. J., 1993, “The effect of applied pressure on the shape of a two-dimensional liquid curtain falling under the influence of gravity”, *Journal Fluid Mechanical*, Vol. 255, 647-665 p.
- Limat L., Jenffer P., Dagens B., Touron E., Fermigier M. and Westfreid J. E., 1992, “Gravitational instabilities of thin liquid layer: dynammics of pattern selection”, *Physica D*, Vol. 61, 166-182 p.

- Lin S. P., Lian Z.W., and Creighton B. J., 1990, "Absolute and convective instability of a liquid sheet", *Journal Fluid Mechanics*, Vol. 220, 673-689 p.
- Roche J. S. and Le Grand N., Brunet P., Lebon L. and Limat L., 2006, "Perturbations on a liquid curtain near break-up: Waves and free edges", *Physics of Fluids*, Vol. 18, 082101/1-13 p.
- Squire H. B., 1993, "Investigation of instability of a moving liquid film", *British Journal Applied Physics*, Vol. 4, 167-169 p.
- Sünderhauf G., Rasziller H. and Durst F., 2001, "The retraction of the edge of a planar liquid sheet", *Physics of Fluids*, Vol.14, No. 1, 198-208 p.
- Teng C. H., Lin S. P., and Chen J.N., 1997, "Absolute and convective instability of a viscous liquid curtain in a viscous gas", *Journal Fluid Mechanics*, Vol. 332, 105-120 p.

## **7. RESPONSIBILITY NOTICE**

The authors are the only responsible for the printed material included in this paper.